Supplementary Information

Construction and mechanism analysis of an ultra-sensitive GCN/Pb^{2+}/PPy heterojunction electrochemiluminescent sensor for detecting Cu (Ⅱ)

Jie Wang[a,b], Yuhui Yi[a], Mu Yang[a,b], Dongyan Tian[a], Jinshan Liu[a], Yu Yu[a,b], Songmei Wu[a,b] and Kejian Ding[a,b]*

[a] School of Physical Science and Engineering, Beijing Jiaotong University, Beijing, 100044, PR China

[b] Beijing Key Laboratory of Novel Materials Genetic Engineering and Application for Rail Transit, Beijing Jiaotong University, Beijing, 100044, PR China

---

*Corresponding Author: Kejian Ding

School of Physical Science and Engineering, Beijing Jiaotong University

Telephone: +86-010-51684352.

E-mail: dkjian@bjtu.edu.cn

Contents:

1.The EDS mapping of Pb^{2+} and Cu^{2+}

To investigate the effect of concentrated hydrochloric acid and the distribution of metal ions, Energy Dispersive X-Ray Spectroscopy (EDS) was employed to test the elemental distribution of GCE/GCN/Pb^{2+}/PPy before hydrochloric acid treatment and after two rounds of experiments. The pre-assembly solution was electropolymerized onto the GCN surface, and uniform distribution of Pb elements could be observed (Figure S1(a)). However, after being soaked with concentrated hydrochloric acid, it was evident that the arrangement of the PPy chains changed, so the lead elements followed the exact distribution change of the PPy chains (Figure S1(b)). The distribution of copper and lead elements was highly coincident, mostly on PPy chains, which indicated that Cu^{2+} recognition should be at the junction of PPy chains and GCN (Figure S1(c)).

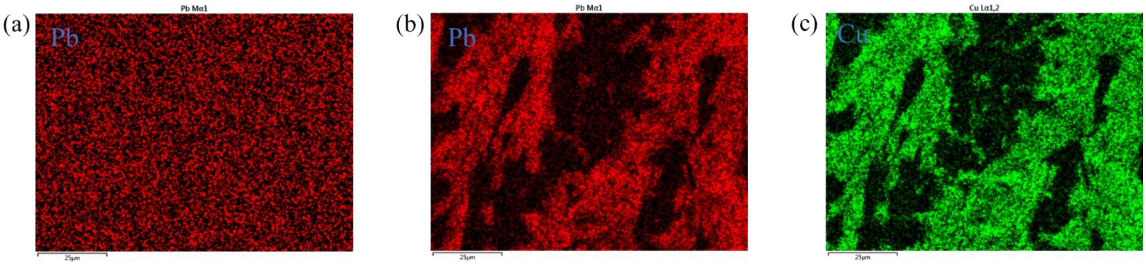

Figure S1. EDS mapping images of GCN/Pb^{2+}/PPy before elution(a) and after detecting Cu^{2+} (b, c).

2. Optimization of experimental conditions

After investigating the possible mechanism of the sensor, we believe that the visible light emitted by the sensor originated from GCN. Moreover, the luminescence intensity of GCN is much higher than that of the sensor. Therefore, the optimization of experimental conditions aimed to increase the luminescence of GCN. The following experimental parameters to be optimized included the concentrations of KCl and $S_2O_8^{2-}$ and the pH of the solution. When the KCl concentration was below 0.1 M, the luminescence intensity of the system increased with the solution conductivity. However, there was no significant luminescence enhancement after the KCl concentration exceeded 0.1 M. Therefore, the sensor's optimal KCl concentration was 0.1 M (Figure S2(a)). $S_2O_8^{2-}$ is the co-reactant of the system. When its concentration was lower than 0.1 M, with the concentration increased the system's luminescence also increased. However, higher than 0.1 M, the luminescence intensity was reduced with the concentration increased, which may be because too much persulfate and other anions in the double electric layer outside formed severe electrostatic repulsion in persulfate ions. And it was not easy to fully participate in the electroluminescence reaction, which reduced the intensity of the ECL. Therefore, the $S_2O_8^{2-}$ concentration chosen for the sensor was 0.1 M (Figure S2(b)). With the pH of the solution from 4.5 to 9, the luminescence of GCN was enhanced and then weakened, probably because alkaline environment had an inhibitory effect on the electron leap of GCN. During the experiment, the luminescence of GCN was most potent at pH 7, so the pH value chosen for the sensor was 7 (Figure S2(c)).

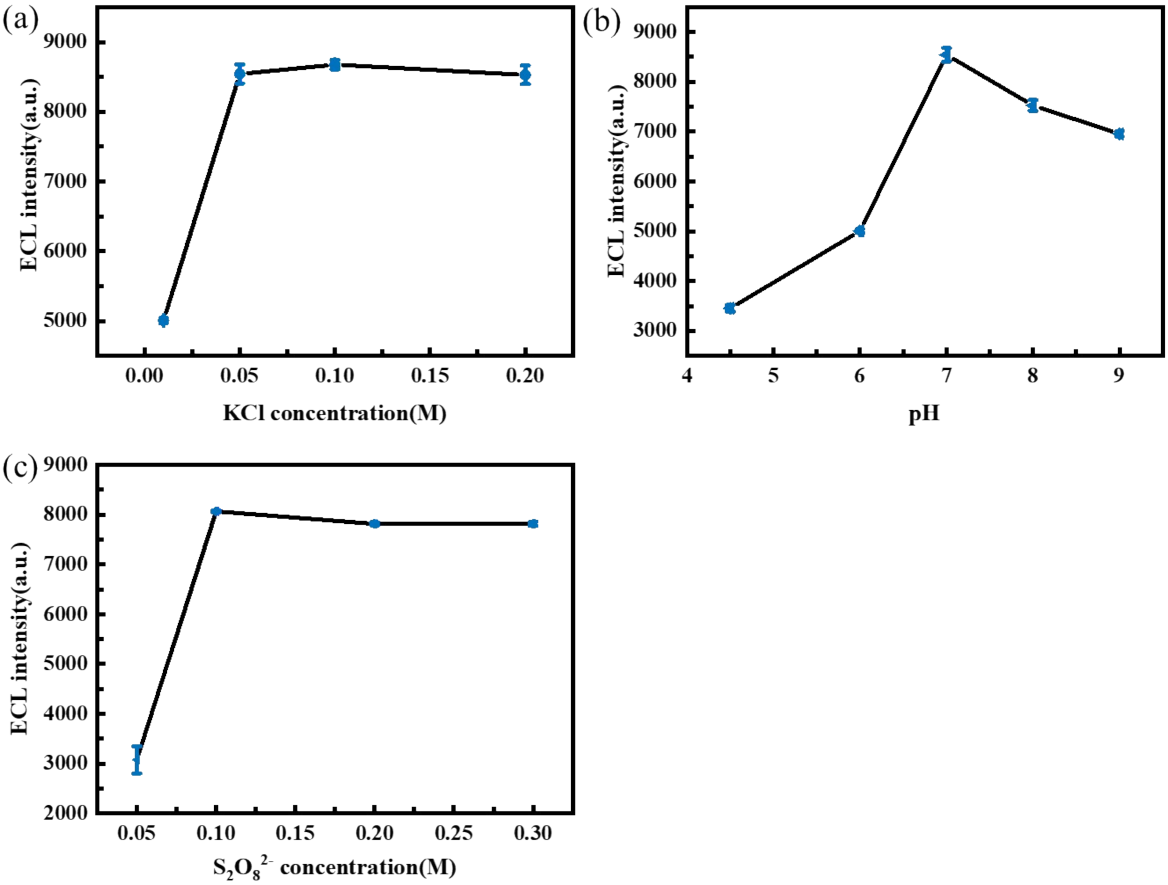

Figure S2. Optimizations of KCl concentration(a), pH(b) and $S_2O_8^{2-}$(c) concentration.

3. Real water sample tests

Here we utilized the heterojunction sensor and ICP-MS machine (Perkin Elmer NexION 300D, USA) to evaluate the concentration of the same samples. It turned out that the results were nearly the same.

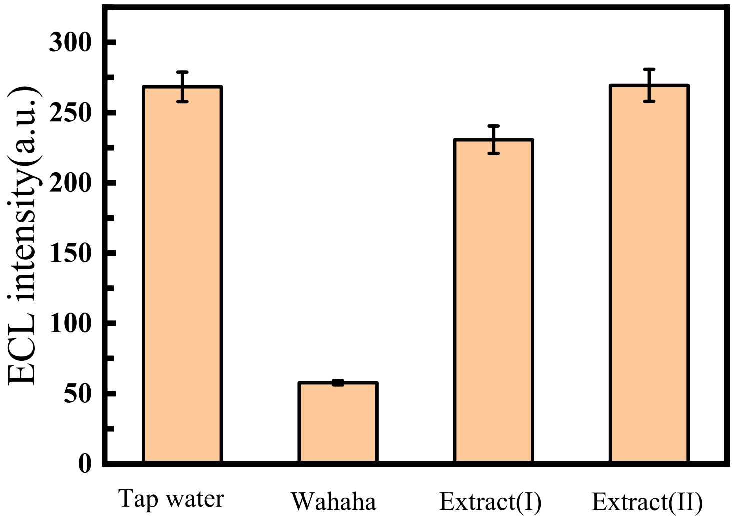

Figure S3. The real water sample test.

4. The reproducibility of the fabricated sensor

The sensor was rinsed several times with Mili-Q water and it still showed an extraordinary reproducibility performance with low RSD as 3%. It means that the sensor was reliable and robust.

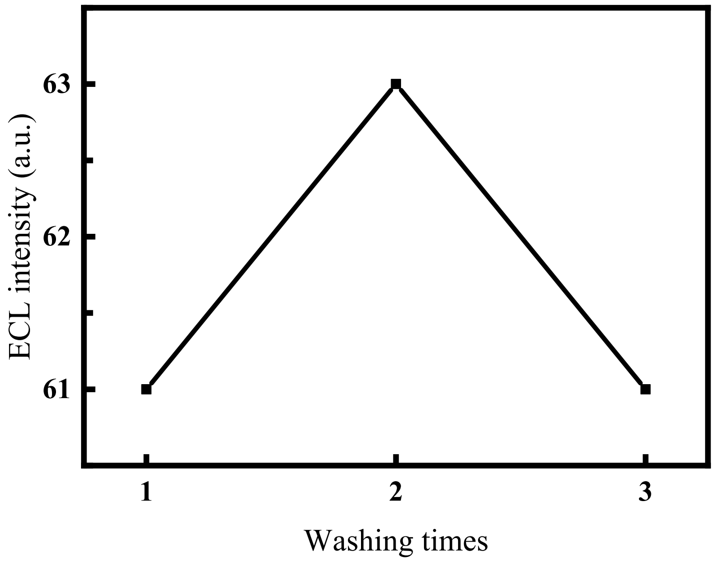

Figure S4. The reproducibility of the fabricated sensor

5.The possible space that Pb elements may exist

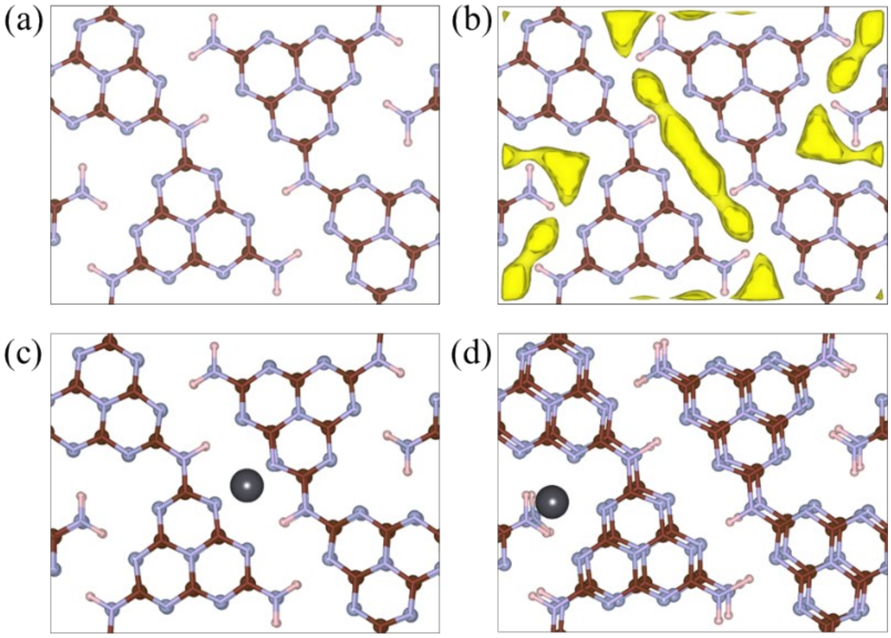

Figure S5. The crystal structure of GCN with $P2_12_12$ space group (a), corresponding free area for a unit cell (b), and possible position for the addition of Pb^{2+} at (c) the center of the unit cell and (d) the space among amino group and heptazine structures. (Brown: C; Blue: N; Pink: H; Black: Pb; Yellow: free area)

6.The orbitals of different processes of detection

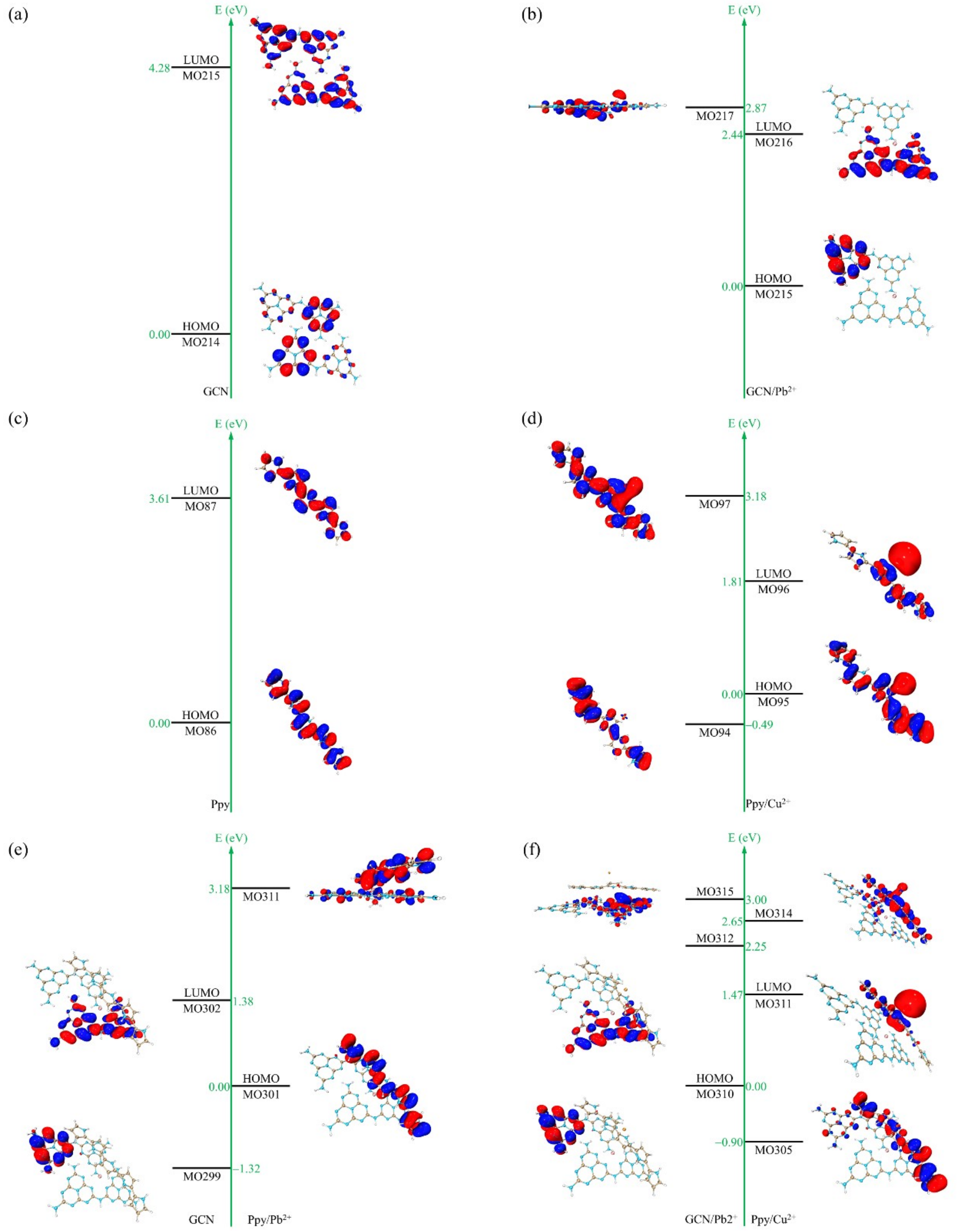

Figure S6. The NBOs of (a) GCN, (b)GCN/Pb^{2+}, (c) PPy, (d) PPy/Cu^{2+}, (e) GCN/PPy/Pb^{2+}, and (f) GCN/Pb^{2+}/PPy/Cu^{2+}. (Green: N; Orange: C; White: H; Pink: Pb; Yellow: Cu)

7. The calculation of the Gibbs Free Energy changes to form a PPy/metal ions structure

To further understand why the sensor could show a better selectivity to Cu^{2+} instead of some other metal ions, Gibbs Free Energy calculation in air and water (corresponding to PPy1, 2) was carried out. Apparently, Fe^{3+} exhibited the lowest ΔG followed by Cu^{2+}. But Fe^{3+} is relatively an active element and can be easily reduced to Fe^{2+}. Therefore, the most possible explanation could be that Cu^{2+} showed the largest adsorption force to the heterojunction material.

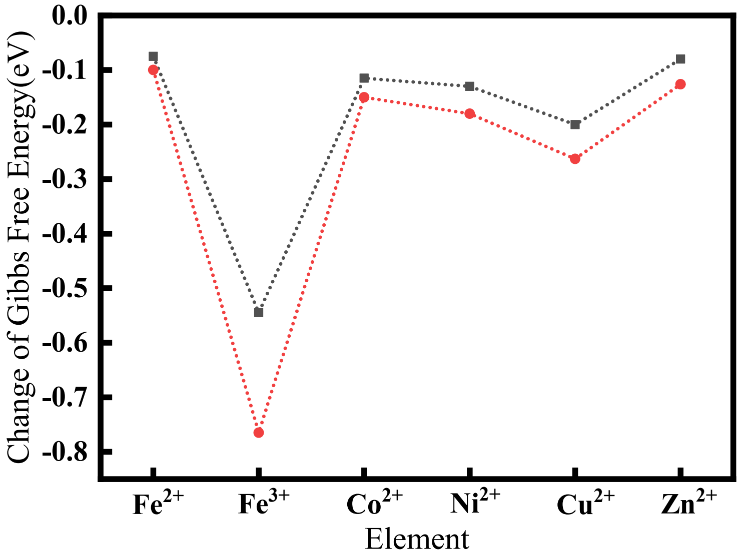

Figure S7. The calculation of the Gibbs Free Energy changes to form a PPy/metal ions structure